Eur. Phys. J. D **32**, 119–128 (2005)
DOI: 10.1140/epjd/e2004-00193-0

THE EUROPEAN PHYSICAL JOURNAL D

Performance of quantum phase gates with cold trapped atoms

A. Negretti[1,2,3,a], T. Calarco[1,2,4], M.A. Cirone[5], and A. Recati[2,4]

[1] ECT*, Villa Tambosi Strada delle Tabarelle 286, 38050 Villazzano, Italy
[2] CRS BEC-INFM and Dipartimento di Fisica, Università degli Studi di Trento, 38050 Povo, Italy
[3] Institut für Physik, Universität Potsdam, 14469 Potsdam, Germany
[4] Institut für Theoretische Physik, Universität Innsbruck, 6020 Innsbruck, Austria
[5] Abteilung für Quantenphysik, Universität Ulm, 89069 Ulm, Germany

Received 9 January 2004 / Received in final form 12 May 2004
Published online 4 January 2005 –

Abstract. We examine the performance of a quantum phase gate implemented with cold neutral atoms in microtraps, when anharmonic traps are employed and the effects of finite temperature are also taken into account. Both the anharmonicity and the temperature are found to pose limitations to the performance of the quantum gate. We present a quantitative analysis of the problem and show that the phase gate has a high quality performance for the experimental values that are presently or in the near future achievable in the laboratory.

PACS. 03.67.Lx Quantum computation – 32.80.Pj Optical cooling of atoms; trapping – 34.90.+q Other topics in atomic and molecular collision processes and interactions

1 Introduction

The implementation of quantum logic gates [1] is a major goal in the current research in quantum information. Several schemes have been proposed in the latest years, based on different physical systems: trapped ions [2] or neutral atoms [3], cavity–QED and photons [4] molecules [5], quantum dots and Josephson junctions [6]. The aim is to implement a fundamental logic quantum gate that works as a constituent block of a quantum computer [7]. One of such gates is the phase gate, whose truth table is

$$\begin{aligned} |a\rangle|a\rangle &\to |a\rangle|a\rangle \\ |a\rangle|b\rangle &\to |a\rangle|b\rangle \\ |b\rangle|a\rangle &\to |b\rangle|a\rangle \\ |b\rangle|b\rangle &\to e^{i\vartheta}|b\rangle|b\rangle. \end{aligned} \tag{1}$$

When $\vartheta = \pi$, this is equivalent — up to a single-qubit rotations — to a controlled-NOT gate. Throughout this paper, we shall assume $\vartheta = \pi$.

Atoms are very good candidates for implementing quantum gates, because of the significant experimental achievements realized in recent years. The techniques to cool and trap charged and neutral atoms have lead to an unprecedented precision in controlling even single atoms. In particular, neutral atoms seem to be the most promising systems for quantum information processing, because the dissipative influence of the environment is relatively weaker when compared to other physical systems.

A proposal for implementing a phase gate with cold neutral atoms stored in microtraps has been recently put forward by Calarco et al. [3]. Two atomic internal states, denoted as $|a\rangle \longmapsto |0\rangle$ and $|b\rangle \longmapsto |1\rangle$, are used as logical states, and the operations that realize the truth table equation (1) involve the external degrees of freedom. Each atom is placed in a microtrap, which can be state–selectively switched off and substituted by a larger harmonic potential that allows collisional interaction between two atoms. The interaction provides the phase that appears in the truth table equation (1). For the sake of simplicity, the traps were assumed to be perfectly harmonic.

In the present article we reexamine this proposal for a phase gate and in contrast to the work in reference [3], we employ, when it is possible and useful, the exact analytic expression of the eigenstates of two harmonic oscillators with contact interaction [8]. Besides, with respect to the harmonic term, we consider the successive terms of the Taylor series expansion of the potential. In particular we focus on the fourth term, which yields the lowest-order correction to the dynamics. The effects of the temperature are also examined. In realistic experimental situations these feature will unavoidably become relevant.

The article is organized as follows: in Section 2 we describe how the quantum phase gate analyzed here can be implemented. We stress that two conditions, (i) full revival of the motional state and (ii) the acquisition of the correct

[a] e-mail: negretti@ect.it

phase shift, are the essential ingredients for a correct performance of the gate. Then Section 2.1 describes how the phase gate can be implemented by using neutral atoms in microtraps and how the two conditions mentioned above can be fulfilled. In Section 3 we examine the performance of the gate when the atoms are at zero temperature and oscillate in harmonic traps. This situation was already investigated numerically in [3], but here we use the exact eigenstates of the problem. The results presented here are in total agreement with those shown in [3]. In Section 4 we examine the performance of the gate when the trap is anharmonic. We obtain quantitative estimates for the quality of the gate performance. In Section 5 we present a heuristic method that, given a certain anharmonicity, improves the performance by choosing the trap parameters in such a way as to optimize the overlap between the initial and the final state. In Section 6 we consider the case when the atoms are at finite temperature and we provide a quantitative measurement of the performance using a definition of the fidelity. In Section 7 we show some connections with our anharmonic model and the physical implementation of the gate on atom chips. Section 8 contains our conclusions.

2 Implementing a phase gate with neutral atoms

A phase gate with the truth table equation (1) can be implemented by employing two internal atomic states (hyperfine states) as the logic values a and b and by making use of the motional degrees of freedom of the atoms to manipulate the qubits. In order to keep the exposition simple, we assume that the atoms are at zero temperature, described by the state

$$\begin{aligned}|\Psi_{\rm AB}(t=0)\rangle &= |\psi_{\rm AB}(0)\rangle \otimes |\chi\rangle \\ &= |\psi_{\rm AB}(0)\rangle(c_a|a_{\rm A}\rangle + c_b|b_{\rm A}\rangle)(c'_a|a_{\rm B}\rangle \\ &\quad + c'_b|b_{\rm B}\rangle) \\ &= |\psi_{\rm AB}(0)\rangle(c_a c'_a|a_{\rm A}\rangle|a_{\rm B}\rangle \\ &\quad + c_a c'_b|a_{\rm A}\rangle|b_{\rm B}\rangle + c_b c'_a|b_{\rm A}\rangle|a_{\rm B}\rangle \\ &\quad + c_b c'_b|b_{\rm A}\rangle|b_{\rm B}\rangle), \end{aligned} \tag{2}$$

where

$$|\chi\rangle \equiv (c_a|a_{\rm A}\rangle + c_b|b_{\rm A}\rangle)(c'_a|a_{\rm B}\rangle + c'_b|b_{\rm B}\rangle) \tag{3}$$

is the general initial internal state of the two atoms, the complex coefficients c_a, c_b, c'_a, c'_b satisfy the normalization conditions $|c_a|^2 + |c_b|^2 = 1$ and $|c'_a|^2 + |c'_b|^2 = 1$, and $|\psi_{\rm AB}(0)\rangle$ is the motional state at $t = 0$. The experimental preparation of the initial state can be made, for example, with a phase transition from a superfluid to a Mott-insulator, so that each atom is located in the ground state of a single well [9]. Then, by means of optical pumping one can initialize the internal state of the atoms. In this way we have an initial state with internal and external states factorized. The phase gate operation is obtained with a sequence of unitary transformations that lead to the final state

$$\begin{aligned}|\Psi_{\rm AB}(t=\tau)\rangle &= |\psi_{\rm AB}(\tau)\rangle(c_a c'_a|a_{\rm A}\rangle|a_{\rm B}\rangle \\ &\quad + c_a c'_b|a_{\rm A}\rangle|b_{\rm B}\rangle + c_b c'_a|b_{\rm A}\rangle|a_{\rm B}\rangle \\ &\quad - c_b c'_b|b_{\rm A}\rangle|b_{\rm B}\rangle) \end{aligned} \tag{4}$$

at $t = \tau$. A comparison between the two expressions (2) and (4) for the initial and final states shows that two ingredients are essential: (i) a sign change must occur only in the last term of equation (4) and (ii) the motional state must be disentangled from the internal states at the end of the gate operations. It is important to stress that during the gate operation the internal states and the external ones are entangled. Thus, we design the dynamics such in a way that at the end of the gate operation ($t = \tau$) the internal states are disentangled from the external states so that a pure logical operation is achieved. These two conditions are fulfilled if the motional state, whose wavefunction is $\psi(x_{\rm A}, x_{\rm B}, t)$, regains its initial form $\psi(x_{\rm A}, x_{\rm B}, 0)$ at some later time τ and acquires a phase π only when both atoms are in the excited state.

2.1 Phase gate with two trapped cold atoms

A natural choice to obtain the recurrence of the initial state $\psi(x_{\rm A}, x_{\rm B}, 0)$ are atoms oscillating in harmonic traps, where full revivals of wave packets are periodically observed for any initial state of a single atom. However, the sign change, i.e., the occurrence of a phase π in the wave packet only if both atoms are internally excited, can be achieved only via an interaction between the atoms that depends on the internal states. This interaction provokes deviations from full revivals of the wave packet and works against a correct performance of the phase gate. The aim of our studies is to investigate under which conditions the complete wave packet revival is at least approximately satisfied, and to evaluate the corresponding gate fidelity.

The system we consider to implement all quantum logic gates is an array of cold bosonic neutral atoms confined in microtraps. Experimentally there are different techniques to trap neutral atoms. As an example, optical dipole traps using holographic techniques [10]. Holographic optical tweezers use a computer designed diffractive optical element to split a single collimated beam into several beams, which are then focused by a high numerical aperture lens into an array of tweezers. Then, by using computer-driven liquid crystal spatial light modulators [11], the optical potential of each trap can be controlled and reconfigured and for instance each site can be moved and switched on and off independently from the others.

Another proposal is based on the employing of micro-optical elements [12]. An array of dipole traps can be obtained by focusing a laser beam into a MOT with an arrays of microlenses, where each trap could be addressed individually. In this case one employs one-dimensional arrays of cylindrical microlenses. A laser beam is sent through such a system and forms a series of parallel focal lines

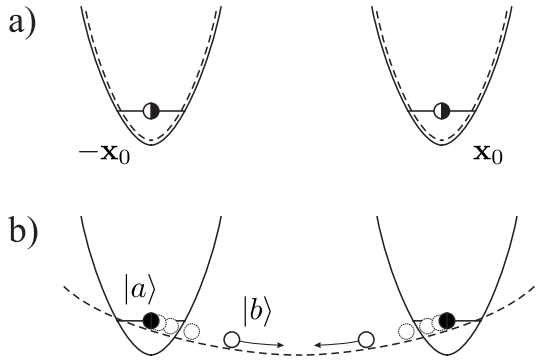

Fig. 1. Configuration at times $t < 0$ and $t > \tau$ (a), and during the gate operation (b). The solid (dashed) curves show the potentials for atoms in internal state $|a\rangle$ ($|b\rangle$).

above the lens array. With a laser detuning below an atomic resonance a one-dimensional array of linear waveguides is formed and atoms are confined in the two dimensions perpendicular to the lens axis. An alternative approach is to use magnetic confinement generated by thin gold wires (1 to 30 μm width) mounted on surfaces (typical materials are silicon, gallium arsenide, aluminum nitride), the so called "atom chips" [13]. The loading of cold atoms into the chip traps can be made in two steps: cool and trap atoms close to the surface in a surface MOT, and transfer the atoms from there to the microtraps on the chip.

We briefly describe how the gate works at temperature $T = 0$. More details can be found in [3]. We assume that bosonic rubidium atoms are employed and use typical experimental values for the parameters. For the sake of simplicity, we focus our attention on only two atoms, under the assumption that we can restrict our analysis to a one-dimensional system. For this purpose a strong harmonic confining potential, with frequency $\omega_\perp$, in the transverse directions y and z can be employed.

According to Figure 1, at $t < 0$ the two atoms are confined in two harmonic microtraps of frequency ω_0, centred at $x = -x_0$ and $x = x_0$, respectively. The distance between the two traps is such that the atoms do not interact each other. At time $t = 0$, the shape of the trapping potential changes for the particles in the state $|b\rangle$ into a common harmonic well of frequency $\omega < \omega_0$, centred at $x = 0$ [dashed line in Fig. 1b], whereas the potentials for the particles in state $|a\rangle$ remain unchanged [solid line in Fig. 1b]. By removing the barrier, particles in state $|b\rangle$ start to oscillate and will collide. As a last step, the atoms have to be restored to the initial motional state of Figure 1a. The whole process of switching potentials is performed through switching the shape of the potential instantaneously at times $t = 0$ and $t = \tau$, where τ is a multiple of the oscillation period in the well of Figure 1b (dashed line).

In order to avoid undesired interactions between the two atoms in different internal states, the atom in the ground state is shifted in the transverse direction. Indeed, this interaction would spoil the performance of the quantum gate, as already discussed in [3]. Only when both atoms are excited they oscillate in the central trap and interact.

For convenience of notation, let us define the following Hamiltonians

$$H_0^- = \frac{p^2}{2M} + \frac{1}{2}M\omega_0^2(x + x_0)^2 \tag{5}$$

$$H_0^+ = \frac{p^2}{2M} + \frac{1}{2}M\omega_0^2(x - x_0)^2 \tag{6}$$

$$H_0 = \frac{p^2}{2M} + \frac{1}{2}M\omega^2 x^2 \tag{7}$$

$$H_{\rm N}^\lambda = H_0 + \frac{M^2\omega^3}{\hbar}\lambda x_{\rm N}^4, \qquad {\rm N} = {\rm A}, {\rm B} \tag{8}$$

$$H_{\rm AB}^\lambda = H_{\rm A}^\lambda + H_{\rm B}^\lambda + 2a_s\hbar\omega_\perp\delta(x_{\rm A} - x_{\rm B}). \tag{9}$$

The Hamiltonians (5) and (6) describe the atoms oscillating in the harmonic microtraps with frequency ω_0, centred in $-x_0$ and x_0, respectively, where the two atoms are placed before the gate operation. The atoms remain in these traps when they are in the internal ground state. The Hamiltonian (7) describes one atom freely oscillating in the central trap with frequency ω. The Hamiltonian (8) describes an anharmonic central trap, derived from the harmonic oscillator Hamiltonian (7) by adding a quartic term, where the dimensionless parameter λ measures the strength of the anharmonicity. The choice of this particular form of the anharmonic trap will be justified in Section 4. Finally, the Hamiltonian (9) describes two atoms in the anharmonic central trap interacting via a contact potential described by the Dirac delta function $\delta(x_{\rm A} - x_{\rm B})$. The coupling strength depends on the three-dimensional scattering length a_s of the two atoms in the internal $|b\rangle$ and on the frequency $\omega_\perp$ [14,15]. We recall that the approximation $2a_s\hbar\omega_\perp\delta(x_{\rm A} - x_{\rm B})$ is valid only for $l_\perp = [\hbar/(M\omega_\perp)]^{1/2} \gg a_s$.

The initial state of the two atoms is

$$|\psi_{\rm AB}(0)\rangle = |\varphi_{0{\rm A}}^-\rangle(c_a|a_{\rm A}\rangle + c_b|b_{\rm A}\rangle) \times |\varphi_{0{\rm B}}^+\rangle(c_a'|a_{\rm B}\rangle + c_b'|b_{\rm B}\rangle) \tag{10}$$

where $\varphi_n^\pm$ denote the eigenstates of $H_0^\pm$. The gate operation is described by a unitary evolution operator $U_{\alpha,\beta}(t)$, which depends on the internal states $\alpha, \beta = a, b$ of the two atoms and transforms the initial state into

$$\begin{aligned}
|\psi_{\rm AB}(t)\rangle &= U_{\alpha,\beta}(t)|\psi_{\rm AB}(0)\rangle \\
&= \left(e^{-i\omega_0 t}|\varphi_{0{\rm A}}^-\rangle\right)\left(e^{-i\omega_0 t}|\varphi_{0{\rm B}}^+\rangle\right)c_a c_a'|a_{\rm A}\rangle|a_{\rm B}\rangle \\
&\quad + \left(e^{-i\omega_0 t}|\varphi_{0{\rm A}}^-\rangle\right)\left(e^{-\frac{i}{\hbar}H_{\rm B}^\lambda t}|\varphi_{0{\rm B}}^+\rangle\right) \\
&\quad \times c_a c_b'|a_{\rm A}\rangle|b_{\rm B}\rangle \\
&\quad + \left(e^{-\frac{i}{\hbar}H_{\rm A}^\lambda t}|\varphi_{0{\rm A}}^-\rangle\right)\left(e^{-i\omega_0 t}|\varphi_{0{\rm B}}^+\rangle\right) \\
&\quad \times c_b c_a'|b_{\rm A}\rangle|a_{\rm B}\rangle \\
&\quad + \left(e^{-\frac{i}{\hbar}H_{\rm AB}^\lambda t}|\varphi_{0{\rm A}}^-\rangle|\varphi_{0{\rm B}}^+\rangle\right)c_b c_b'|b_{\rm A}\rangle|b_{\rm B}\rangle
\end{aligned} \tag{11}$$

at a later time t. Here the anharmonicity of the central trap has been taken into account. The state equation (11)

is in general no longer a separable state of motional and internal degrees of freedom. However, in the present scheme the separation between the states of the motional and internal degrees of freedom can be realized to a good approximation. Indeed, the state

$$|\psi^{aa}_{\rm AB}(t)\rangle \equiv \left(e^{-i\omega_0 t}|\varphi^{-}_{0\rm A}\rangle\right)\left(e^{-i\omega_0 t}|\varphi^{+}_{0\rm B}\rangle\right) \qquad (12)$$

describes two harmonic oscillators in two well-separated microtraps and has therefore full revivals with period $T^0_{osc} \equiv 2\pi/\omega_0$ for any initial state. The states

$$|\psi^{ab}_{\rm AB}(t)\rangle \equiv \left(e^{-i\omega_0 t}|\varphi^{-}_{0\rm A}\rangle\right)\left(e^{-\frac{i}{\hbar}H^{\lambda}_{\rm B}t}|\varphi^{+}_{0\rm B}\rangle\right) \qquad (13)$$

and

$$|\psi^{ba}_{\rm AB}(t)\rangle \equiv \left(e^{-\frac{i}{\hbar}H^{\lambda}_{\rm A}t}|\varphi^{-}_{0\rm A}\rangle\right)\left(e^{-i\omega_0 t}|\varphi^{+}_{0\rm B}\rangle\right) \qquad (14)$$

describe one atom in the microtrap and the other in the central trap. In this case, the atom in the microtrap is shifted in the transverse direction in order to avoid undesired interaction between the atoms. Therefore, if the central trap is harmonic ($\lambda = 0$), full revivals of the two wave packets at different periods occur.

The state

$$|\psi^{bb}_{\rm AB}(t)\rangle \equiv \left(e^{-\frac{i}{\hbar}H^{\lambda}_{\rm AB}t}|\varphi^{-}_{0\rm A}\rangle|\varphi^{+}_{0\rm B}\rangle\right) \qquad (15)$$

is affected by the interaction between the atoms in the wide trap. This interaction is necessary in order to yield the sign change for the phase gate operation but it also modifies the atomic wave packet. For a good performance of the quantum gate the modification must be small. The overlap fidelity

$$O(\psi^{bb}_{\rm AB}, t) \equiv \quad \langle\psi^{bb}_{\rm AB}(t)|\psi_{\rm AB}(0)\rangle \qquad (16)$$

between the initial motional state $|\psi_{\rm AB}(0)\rangle$ and that at a later time $t > 0$, $|\psi^{11}_{\rm AB}(t)\rangle$ gives an estimate of the quality of the gate performance. If the revival of the motional state is nearly complete at $t = \tau$, it results

$$|O(\psi^{bb}_{\rm AB}, \tau)|^2 \simeq 1. \qquad (17)$$

Under this condition, we can write the motional state at time τ as

$$|\psi^{bb}_{\rm AB}(\tau)\rangle \simeq e^{-i\phi_{bb}(\tau)}|\psi_{\rm AB}(0)\rangle \qquad (18)$$

where $\phi_{bb}(\tau)$ denotes the phase of the motional wave function. When

$$\phi_{bb}(\tau) = \pi, 3\pi, 5\pi, \ldots, \qquad (19)$$

the phase gate operation is correctly realized. In the next sections we investigate when the two conditions of full or nearly full revival (expressed by Eq. (17)) of the motional state of the excited atoms and the acquisition of the correct phase (expressed by Eq. (19)) are satisfied.

3 Ideal case: two cold atoms in harmonic traps

We examine first the performance of the quantum phase gate when all traps are harmonic. This ideal situation was already investigated in [3], but we examine it again, because here we use the exact solutions of the Schrödinger equation for this problem. Indeed, it has been recently found that the problem of two interacting atoms in one harmonic trap has an exact solution in one, two and three dimensions [8]. Here we simply summarize the results for one dimension. It is useful to define the new coordinates $X \equiv (x_{\rm A} + x_{\rm B})/\sqrt{2}$ and $x \equiv (x_{\rm A} - x_{\rm B})/\sqrt{2}$. The pseudo–particle described by the centre of mass coordinate X is a free harmonic oscillator, with eigenstates $\varphi_n(X)$ and energy $E_n = \hbar\omega(n + 1/2)$. The pseudo–particle described by the relative coordinate x describes a harmonic oscillator that feels the contact potential at the origin $x = 0$. Its eigenstates split into two subsets, depending on the function parity. The odd eigenstates are still those of the free harmonic oscillator, since the contact potential acts only at $x = 0$, where the odd wave functions vanish. The even solutions

$$\varphi_\nu(x) \equiv B_\nu \left(\frac{M\omega}{\hbar}\right)^{1/4} \exp\left[-\frac{M\omega}{2\hbar}x^2\right] U\left(-\nu, \frac{1}{2}; \frac{M\omega}{\hbar}x^2\right) \qquad (20)$$

have energy $E_\nu \equiv \hbar\omega(2\nu + 1/2)$, and the function U is the confluent hypergeometric function [16]. Here the real parameters ν are solution of the transcendental equation

$$\frac{\Gamma(1/2 - \nu)}{\Gamma(-\nu)} = -\frac{1}{\sqrt{2}}\frac{a_s}{a_x}\frac{\omega_\perp}{\omega} \qquad (21)$$

where $a_x \equiv \sqrt{\hbar/(M\omega)}$ is the characteristic length associated with the central trap and the normalization coefficients

$$B_\nu = \sqrt{\frac{\Gamma(1/2 - \nu)\Gamma(-\nu)}{\pi[\psi(1/2 - \nu) - \psi(-\nu)]}} \qquad (22)$$

are defined with the help of the logarithmic derivative ψ of the gamma function.

With the help of these exact eigenstates we evaluate the fidelity equation (17) and the phase shift equation (19) when both atoms are excited. At $t < 0$ the two atoms are in the motional ground states of their own microtrap, say, atom A in the left trap, centred at $x = -x_0$, and atom B in the right trap, centred at $x = x_0$. At $t = 0$ the microtraps are switched off, the central trap is switched on and both atoms oscillate in the same trap and interact. In order to calculate the overlap fidelity equation (17), we can proceed in two different but equivalent ways. Since the atoms are identical, the gate performs correctly even when the two atoms end up in the other trap at the end of the operation. We can therefore either symmetrize the initial wave function for the two bosonic atoms, or estimate the overlap fidelity equation (17) as the sum of the probabilities to find the (distinguishable) atoms in the original traps or with the initial positions interchanged. Since in this section we use the wave functions of the center of mass X

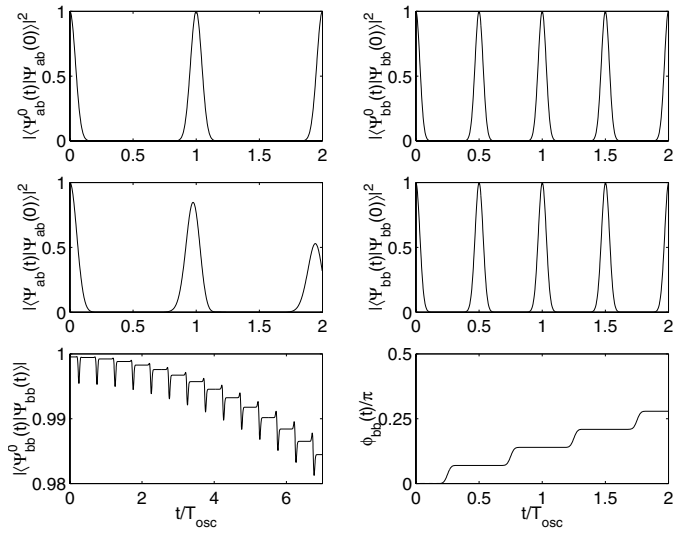

Fig. 2. Dynamics during gate operation: projection of the initial state on the state evolved without (top) and with interaction (center); projection of the evolved state on the corresponding state evolved without interaction (bottom left) and interaction-induced phase shift (bottom right). We choose $\omega = 2\pi\times 17.23$ kHz and $\omega_\perp = 2\pi\times 150$ kHz with the initial wells having a frequency $\omega_0 = 2\omega$ and displaced by $x_0 = 410$ nm. This reproduces analytically the results obtained in [3] with a purely numerical approach.

and of the relative coordinate x, the first approach is more convenient. The two-atom motional state at generic time $t > 0$ is

$$\psi(X, x, t) = \sum_{n,\nu} c_{n,\nu} e^{-i(n+2\nu+1)\omega t} \varphi_n(X)\varphi_\nu(x) \qquad (23)$$

where the odd eigenstates of the relative coordinate x are not included since they describe fermions. The coefficients $c_{n,\nu}$ vanish when n is odd, otherwise

$$c_{n,\nu} = 2\pi^{-1/4}\sqrt{\frac{\omega_0}{n(\omega_0+\omega)}} e^{-\frac{M\omega_0 x_0^2}{\hbar}} 2^{-n/2} \times \frac{\sqrt{n!}}{(n/2)!}\left(\frac{\omega-\omega_0}{\omega+\omega_0}\right)^{n/2} B_\nu \mathcal{I}_\nu \qquad (24)$$

where

$$\mathcal{I}_\nu = \int_{-\infty}^{\infty} dy e^{-\left(1+\frac{\omega_0}{\omega}\right)\frac{y^2}{2}} U\left(-\nu, 1/2; y^2\right) \times \cosh\left[x_0\omega_0\sqrt{\frac{2M}{\hbar\omega}}y\right]. \qquad (25)$$

In Figure 2 we show the overlap fidelity, equation (17). The revival of the motional state, occurs with periodicity $T_{osc}/2$. Indeed, after this period the two atoms are in $x = \pm x_0$. The revival is nearly complete, as the overlap fidelity approaches the value 0.99. In Figure 2 we also report the situation in which atoms in different internal states feel a contact potential in order to show what happens.

In Figure 2 we show the phase shift $\phi_{bb}(\tau)$ due to the interaction. There is a fast change of the phase between the two revivals, in correspondence to the presence of the two atoms at the bottom of the trap, where the interaction occurs. The figure suggests that one can assume that at each interaction there is a jump in the phase. Therefore, after a suitable number of collisions, the motional state acquires the correct phase for the gate operation. The exact results shown here confirm the validity and accuracy of the results of reference [3] obtained numerically.

4 Phase gate performance with anharmonic traps

The operation of the phase gate relies on several simplifying assumptions. In the previous section we have assumed that the atoms are at zero temperature and oscillate in harmonic traps. The experimental conditions are necessarily less ideal and the problem of estimating the effect of deviations from the ideal conditions is particularly important. Among the causes that can lead to bad performance of the phase gate, we mention random noise, caused by fluctuating electromagnetic fields, temperature effects and anharmonicity of the trapping potentials. In particular, some anharmonicity might more easily appear in the wider central trap and seems to be the most important disturbance to be taken into account.

In this section we study the gate performance when the excited atoms oscillate in an anharmonic trap, as described by the Hamiltonians equations (8) and (9). Indeed, independently of its exact expression, we can expand the trapping potential in Taylor series. The first correction to the harmonic approximation is a cubic term, that we shall neglect since at first order of approximation it does not lead to any correction to the energy and it does not affect the atomic motion.

The next relevant correction to the harmonic trap is a quartic term. It is symmetric and it is responsible for an energy shift. We neglect the other terms in the Taylor expansion, which yield minor perturbations. The atom dynamics in the central trap is then described by the Hamiltonians (8) and (9).

The atomic wave packet does no longer show full revivals. Moreover, the partial revivals of the initial state that still occur are no longer periodic, in a strict sense. Therefore, the question arises as to how much anharmonicity can be tolerated without destroying the good performance of the phase gate.

4.1 Anharmonic trap: overlap fidelity for the internal states $|a_A\rangle|b_B\rangle$ and $|b_A\rangle|a_B\rangle$

In this subsection we examine the performance of the gate when only one atom is in the internal excited state. During the gate operation the excited atom (atom A in the left trap, say) oscillates freely in the central anharmonic trap, while atom B oscillates as a free harmonic oscillator in its microtrap. We need only to focus our attention on the

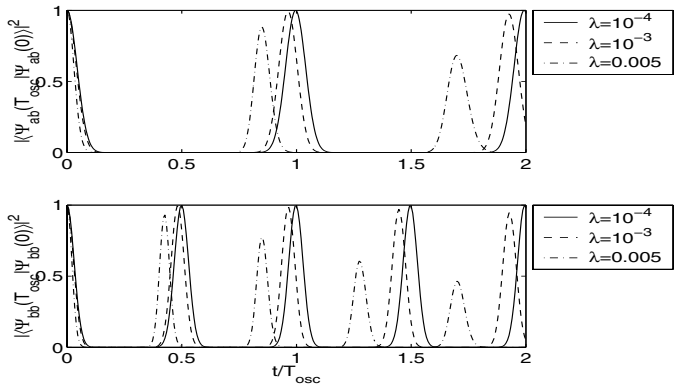

Fig. 3. Dynamics during gate operation: projection of the initial state on the state evolved with different values of anharmonicity. Trap parameters have the same values as in Figure 2.

motion of atom A, whose vibrational state at time t can be expanded on eigenstates of the harmonic oscillators according to

$$|\psi_{\rm A}(t)\rangle = \sum_n c_n(t) e^{-i2\pi nt} |\varphi_{n{\rm A}}\rangle \qquad \left(t \longrightarrow \frac{t}{T_{osc}}\right) \quad (26)$$

where φ_n denotes the eigenstates of H_0 and T_{osc} is the period of oscillation of the central trap [dashed line in Fig. 1b]. The expansion coefficients $c_k(t)$ satisfy the differential equations

$$\begin{aligned}\dot{c}_n(t) = -i\frac{\pi}{2}\lambda\Big\{ & \sqrt{(n+1)(n+2)(n+3)(n+4)}c_{n+4}(t)e^{-i8\pi t} \\ & +2(2n+3)\sqrt{(n+1)(n+2)}c_{n+2}(t)e^{-i4\pi t} \\ & +3\left[(n+1)^2+n^2\right]c_n(t) \\ & +2(2n-1)\sqrt{(n-1)n}c_{n-2}(t)e^{i4\pi t} \\ & +\sqrt{(n-3)(n-2)(n-1)n}c_{n-4}(t)e^{i8\pi t}\Big\}. \end{aligned} \quad (27)$$

The overlap fidelity is

$$\begin{aligned}|O^{ba}(t)|^2 &\equiv |\langle\varphi^-_{0{\rm A}}|e^{-\frac{i}{\hbar}H^\lambda_{\rm A}t}|\varphi^-_{0{\rm A}}\rangle|^2 \\ &= |\sum_k c_k(t)e^{-i2\pi kt}c^*_k(0)|^2 \end{aligned} \quad (28)$$

where

$$c_k(0) \equiv \langle\varphi_{k{\rm A}}|\varphi^-_{0{\rm A}}\rangle. \quad (29)$$

The overlap fidelity (16) has been evaluated numerically and is plotted in Figure 3 on the top for different values of the parameter λ. It is evident from the figure that the gate tolerates some anharmonicity, with a threshold value of the order of $\lambda \sim 10^{-4}$. The specular case of atom B excited, while atom A is not excited, gives the same results.

4.2 Anharmonic trap: overlap fidelity for the internal state $|b_{\rm A}\rangle|b_{\rm B}\rangle$

Here we examine the performance of the gate when both atoms are excited. We expand the motional state of the two atoms on the eigenstates of the central harmonic trap

$$|\psi_{\rm AB}(t)\rangle = \sum_{k,l} c_{k,l}(t)e^{-i2\pi(k+l)t}|\varphi_{k{\rm A}}\rangle|\varphi_{l{\rm B}}\rangle \qquad \left(t \longrightarrow \frac{t}{T_{osc}}\right) \quad (30)$$

and the expansion coefficients $c_{k,l}(t)$ satisfy the equations

$$\begin{aligned}\dot{c}_{k,l}(t) = & -i4\frac{\omega_\perp}{\omega}a_s\sqrt{\frac{m\omega}{\hbar}}e^{i(k+l)2\pi t} \\ & \times\sum_{n,m} c_{n,m}(t)e^{-i(n+m)2\pi t}A_{klnm} \\ & -i\frac{\pi}{2}\lambda\Big[\sqrt{k(k-1)(k-2)(k-3)}\,c_{k-4,l}(t)e^{8i\pi t} \\ & +(4k-2)\sqrt{k(k-1)}c_{k-2,l}(t)e^{4i\pi t} \\ & +(6k^2+6k+3)c_{k,l}(t) \\ & +(4k+6)\sqrt{(k+1)(k+2)}c_{k+2,l}(t)e^{-4i\pi t} \\ & +\sqrt{(k+1)(k+2)(k+3)(k+4)}c_{k+4,l}(t)e^{-8i\pi t} \\ & +\sqrt{l(l-1)(l-2)(l-3)}c_{k,l-4}(t)e^{8i\pi t} \\ & +(4l-2)\sqrt{l(l-1)}c_{k,l-2}(t)e^{4i\pi t} \\ & +(6l^2+6l+3)c_{k,l}(t) \\ & +(4l+6)\sqrt{(l+1)(l+2)}c_{k,l+2}(t)e^{-4i\pi t} \\ & +\sqrt{(l+1)(l+2)(l+3)(l+4)}c_{k,l+4}(t)e^{-8i\pi t}\Big] \end{aligned} \quad (31)$$

where

$$\begin{aligned}A_{klnm} \equiv & \frac{1}{\sqrt{2^{k+l+n+m}}\sqrt{k!l!n!m!}} \\ & \times\int_{-\infty}^{\infty} d\xi e^{-2\xi^2}H_k(\xi)H_l(\xi)H_n(\xi)H_m(\xi) \end{aligned} \quad (32)$$

and H_n denotes the Hermite polynomial of order n. The first term in equation (31) comes from the contact interaction between the two atoms, whereas the other terms are due to anharmonicity. Assuming that the atoms are distinguishable, the overlap fidelity is

$$\begin{aligned}O^{bb}(t) &= \left|\left\langle\varphi^-_{0A}\varphi^+_{0B}\left|e^{-\frac{i}{\hbar}H^\lambda_{AB}t}\right|\varphi^-_{0A}\varphi^+_{0B}\right\rangle\right|^2 \\ &\quad +\left|\left\langle\varphi^+_{0A}\varphi^-_{0B}\left|e^{-\frac{i}{\hbar}H^\lambda_{AB}t}\right|\varphi^-_{0A}\varphi^+_{0B}\right\rangle\right|^2 \\ &= \left|\sum_{kl} c_{kl}(t)e^{-ik2\pi t}e^{-il2\pi t}c^{AB*}_{kl}(0)\right|^2 \\ &\quad +\left|\sum_{kl} c_{kl}(t)e^{-ik2\pi t}e^{-il2\pi t}c^{BA*}_{kl}(0)\right|^2 \end{aligned} \quad (33)$$

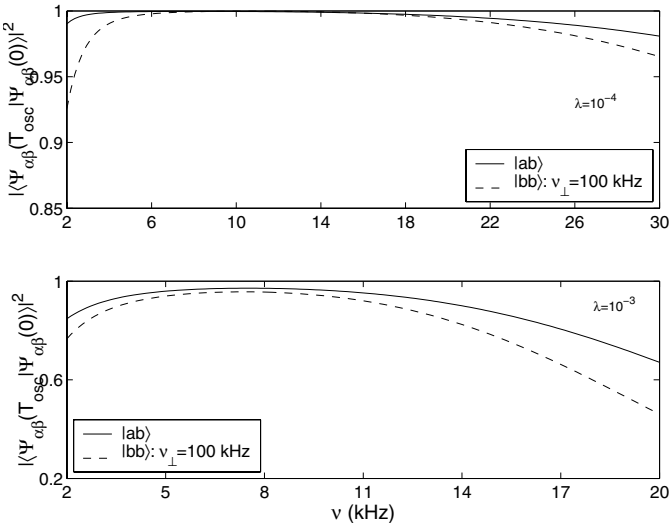

Fig. 4. Overlaps $|O(\psi_{\alpha\beta},\tau)|$ in order to optimize the performance of the phase gate.

where we have defined

$$c_{kl}^{AB*}(0) \equiv \langle \varphi_{0A}^{-}\varphi_{0B}^{+}|\varphi_{kA}\varphi_{lB}\rangle$$
$$c_{kl}^{BA*}(0) \equiv \langle \varphi_{0A}^{+}\varphi_{0B}^{-}|\varphi_{kA}\varphi_{lB}\rangle. \quad (34)$$

We have numerically evaluated the overlap fidelity, which is shown in Figure 3 on the bottom for different values of the parameter λ. Also in this case we see that an anharmonicity of the order of $\lambda \sim 10^{-4}$ or less does not prejudicate the performance of the phase gate.

In conclusion of this section, we note that different choices of the values of the parameters lead to very different performance qualities. For a fixed value of the anharmonicity parameter λ different gate performances are obtained for different values of the other parameters. From the first term on the right hand side of equation (31) one sees that the effect of the contact interaction on the atom dynamics depends on the value of $\omega_\perp/\omega a_s\,(M\omega/\hbar)^{1/2}$. If this quantity is larger than $\approx$0.7, it spoils the occurrence of full revivals; if it is too small, too many oscillations are needed to create the phase $\phi_{bb}(t)=\pi$. We also note that the frequency $\omega_\perp$ must be large enough to prevent excitations along the transverse direction ($l_\perp \gg a_s$). In spite of these limitations, it is possible to find reasonable values for these parameters that make a correct performance possible, as the data in Figure 3 (bottom) show.

5 Optimization of gate performance

The gate perfomance can be optimized reducing the number of oscillations and selecting the trap frequencies $\omega(\lambda)$ and $\omega_\perp(\lambda)$ such that the overlaps $|O(\psi_{\alpha\beta},\tau)|$ are close to one. In this way we have two effects: better performance and faster gate. In Figure 4 we report the overlaps $|O(\psi_{\alpha\beta},\tau)|$ for two different anharmonic situations.

In Table 1 we report the values that optimize the performance.

Table 1. Trap frequencies maximizing the fidelity curves in Figure 4.

λ	ω (kHz)	ω_0 (kHz)	$\omega_\perp$ (kHz)
10^{-4}	$2\pi \times 12.00$	$4\times\omega$	$2\pi \times 769.00$
10^{-3}	$2\pi \times 7.50$	$4\times\omega$	$2\pi \times 517.01$

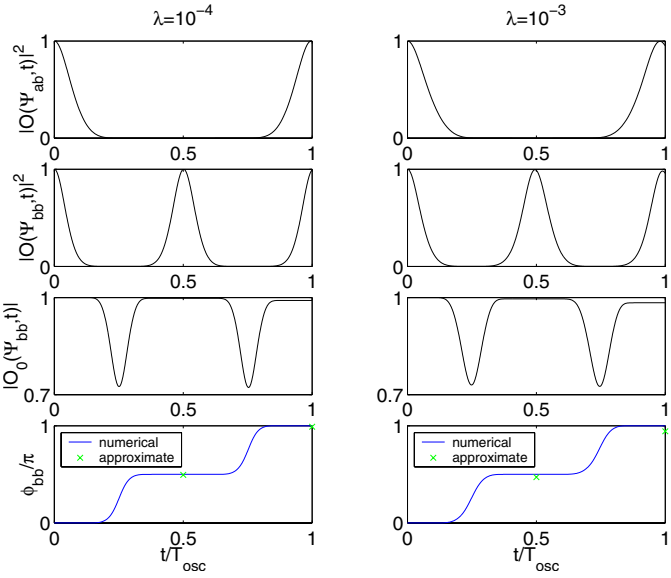

Fig. 5. Dynamics during gate operation: projection of the initial state on the evolved state with interaction (first two rows); projection of the evolved state on the corresponding state evolved without interaction (third row) and interaction-induced phase shift (bottom). The displacement of the two initial separated wells is the same as in Figure 2.

With these values we obtain the results shown in Figure 5. The crosses in the bottom pictures of Figure 5 are obtained by means of these two assumptions: (i) the particles move against each other, come in contact during a certain time interval $[t_i,t_F]$ and then separate again; and (ii) the velocity of each particle and the shape of its wave function do not vary during the interaction. It follows that (see Ref. [3] for more details)

$$\phi_{bb}(T_{osc}) = 2\frac{\omega_\perp a_s}{\omega v} \quad (35)$$

in harmonic oscillator units. Here the velocity v is a positive constant value given by

$$v = |\partial_t \langle\psi_\pm(t)|x|\psi_\pm(t)\rangle|_{t=t_k}|$$
$$= 2\mathcal{R}\Bigg\{\sum_n \overline{c_n(t_k)}E_n^0\left[\sqrt{\frac{n+1}{2}}c_{n+1}(t_k) - \sqrt{\frac{n}{2}}c_{n-1}(t_k)\right]$$
$$+ i\lambda\sum_{n,q}\overline{c_n(t_k)}c_q(t_k)\,e^{i(n-q)\frac{\pi}{2}}\left[\sqrt{\frac{n+1}{2}}\mathcal{I}_{n+1,q}^4 + \sqrt{\frac{n}{2}}\mathcal{I}_{n-1,q}^4\right]\Bigg\},$$

where $\mathcal{I}^4_{n+1,q}$ and $\mathcal{I}^4_{n-1,q}$ are given by

$$\mathcal{I}^s_{n,q} = \left[2^{n+q} n!q!\pi\right]^{-1/2} \int_{-\infty}^{+\infty} dx e^{-x^2} x^s H_n(x) H_q(x), \tag{36}$$

whereas the coefficients $c_n(t)$ are given by equation (27) and $t_k = (2k+1)\,T_{osc}/4$ with k an integer.

Figure 5 shows that there is a good agreement between the numerical result (solid line) and that given by equation (35). The agreement is not perfect, though, simply because the velocity is not constant during the interaction.

6 Gate performance in anharmonic traps at finite temperature

Now we examine the gate performance when both anharmonicity and temperature effects are taken into account. Since the atoms are not in the ground state of the initial trapping potential and therefore their temperature $T \neq 0$, it follows that, for a finite temperature T, the initial state of the two atoms is described by the density matrix

$$\rho_0 = \frac{1}{Z} \sum_{k,l=0}^{\infty} P_{k,l}(T) |\varphi^-_{k\mathrm{A}}\rangle |\varphi^+_{l\mathrm{B}}\rangle \otimes \langle\varphi^-_{k\mathrm{A}}| \langle\varphi^+_{l\mathrm{B}}| \tag{37}$$

where the occupation probabilities of the k and l states are calculated assuming, for each atom, a thermal distribution corresponding to temperature T, as expressed by

$$P_{k,l}(T) \equiv \exp\left[-\frac{\hbar\omega_0}{k_B T}(k+l)\right] \tag{38}$$

and

$$Z = \sum_{k,l=0}^{\infty} P_{k,l}(T) \tag{39}$$

is the canonical partition function.

6.1 Gate fidelity

The most general logical input state has the form

$$|\chi\rangle = \sum_{\alpha,\beta=0}^{1} c_{\alpha\beta} |\alpha,\beta\rangle, \tag{40}$$

which is an arbitrary superposition of all two-qubit computational basis states. The goal of gate operation is to obtain the ideal output

$$|\tilde{\chi}\rangle = \sum_{\alpha,\beta=0}^{1} c_{\alpha\beta} e^{i\phi_{\alpha\beta}} |\alpha,\beta\rangle. \tag{41}$$

This is equivalent to the desired two-qubit transformation equation (1): provided that $\vartheta = \phi_{00} + \phi_{11} - \phi_{01} - \phi_{10}$, the one can be recovered from the other by redefining the logical states via qubit rotations.

Since in this case the two atoms are described by a density matrix, we cannot use the overlap fidelity condition equation (17) to estimate the performance of the phase gate. We use therefore the minimum fidelity [17] to characterize the quality of the phase gate performance [3],

$$\begin{aligned} F &= \min_{\chi} F(\chi) \\ &= \min_{\chi} \langle\tilde{\chi}|\mathrm{Tr}_{\mathrm{ext}}[\mathcal{U} S(\rho_{\mathrm{int}} \otimes \rho_0) S^\dagger \mathcal{U}^\dagger]|\tilde{\chi}\rangle. \end{aligned} \tag{42}$$

Here $\rho_{\mathrm{int}} = |\chi\rangle\langle\chi|$ is the density matrix of the internal state equation (3) and S denotes an operator that symmetrizes the atomic state. If we write

$$|\chi\rangle = \sum_{n=0}^{3} c_n |n\rangle \tag{43}$$

and assume

$$\mathcal{U}\left[|n\rangle \otimes \rho\right] \approx |n\rangle \otimes \mathcal{U}\left[\rho\right], \tag{44}$$

the fidelity takes the form

$$F = \min_{\{c_n\}} \sum_{n,k} |c_n|^2 |c_k|^2 T_{nk}, \tag{45}$$

where

$$T_{nk} = e^{i(\phi_n - \phi_k)} \sum_{n_1,n_2} P_{n_1 n_2}(T) \langle n_2, n_1 | \mathcal{U}^\dagger_n \mathcal{U}_k | n_1, n_2\rangle. \tag{46}$$

The minimum of the fidelity $F(\chi)$ is evaluated in the Appendix. For the ideal case, that is, without anharmonicity but with the exact solutions given by (20), the fidelity at $T = 0$ is $F \approx 0.99$.

Table 2. Fidelity at $T = 0$ for two values of anharmonicity.

λ	F
10^{-4}	0.99
10^{-3}	0.97

In Table 2 we show the values of the fidelity at zero Kelvin with the frequencies given in Table 1, which optimizes the fidelity, for different values of the anharmonicity. It is important to note that these results are obtained considering $\tau = T_{osc}$ instead of $\tau = 7T_{osc}$ as in reference [3], in order to improve the gate time operation.

When the atoms are at finite temperature, the fidelity decreases. If we define $\gamma = \exp\left[-\hbar\omega_0/\left(k_B T\right)\right]$ and evaluate (46) neglecting terms of the order $O\left(\gamma^3\right)$ the fidelity turns out to be $F \approx 0.97$ for $\lambda = 10^{-4}$ at $T \approx 0.5$ μK. In Figure 6 we show the behavior of the fidelity with the temperature for $\lambda = 10^{-4}$ and $\lambda = 10^{-3}$.

It is important to highlight that, since different values of λ lead to different optimal trap frequencies $\omega_0(\lambda)$, the curves in Figure 6 are plotted as a function of the ratio $k_B T/(\hbar\omega_0(\lambda))$. Thus, e.g., the maximum value of the

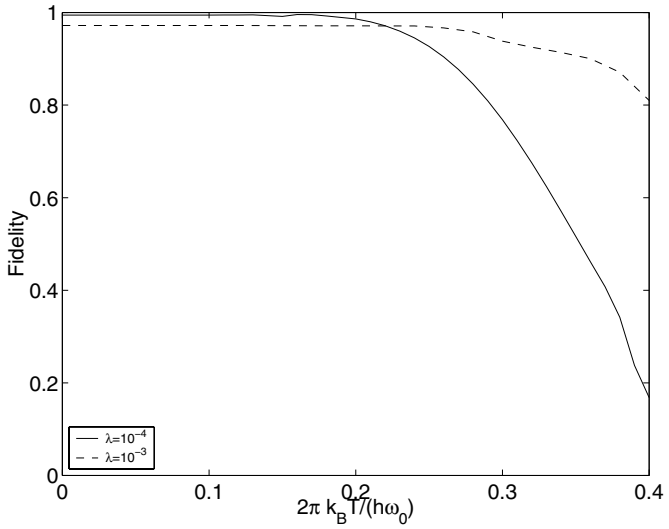

Fig. 6. Fidelity F against temperature $k_BT/(\hbar\omega_0(\lambda))$ for ^{87}Rb. Trap parameters have the values given in Table 1.

x-axis of the $\lambda = 10^{-4}$ curve corresponds at a temperature of the order of about 1 μK and for $\lambda = 10^{-3}$ is 0.1 μK, an order of magnitude smaller.

7 Estimating λ in a realistic situation

We show how λ is related to the trap's parameters and the properties of the atoms used in actual experiments where magnetic traps are used for the confinement of neutral atoms. The interaction between the magnetic dipole moment of an atom in some hyperfine state $|F, m_F\rangle$ and an external magnetic field $\mathbf{B}$ is

$$H_{\rm int} = -\boldsymbol{\mu} \cdot \mathbf{B}. \tag{47}$$

In an inhomogeneous magnetic field, if the atomic motion is slow as compared with the velocity of change of the field vector as seen by the moving atom, the interaction only depends on the absolute value of the field:

$$H_{\rm int} = -\mu_z B = g_F m_F \mu_B B, \tag{48}$$

where μ_B is the Bohr magneton and g_F is the Landé factor. As in [3], we consider here an atomic mirror like the one realized [18,19] from a solid-state magnetic medium with permanent sinusoidal magnetization $\mathbf{M} = (M_0 \cos[k_M x, 0, 0])$ along the x-axis. In order to avoid trap losses, due to spin flips occurring at magnetic field zeros [20], it is necessary to apply a certain external bias field B_2 along the y-direction. Moreover, to obtain a corrugation in the magnetic field modulus, we add a rotating external field B_1 in the xz-plane, at an angle θ with the surface that can be varied at will. In this case the magnetic trapping potential is

$$V_{m_F}(\mathbf{x}) = g_F \mu_B m_F \left\{ \left[B_0 e^{-z k_M} \cos^2(k_M x) + B_1 \cos\theta \right]^2 + \left[B_0 e^{-z k_M} \sin^2(k_M x) + B_1 \sin\theta \right]^2 + B_2^2 \right\}^{1/2} \tag{49}$$

where $B_0 = \mu_0 M_0 \left(1 - e^{-k_M \delta}\right)/2$ and δ is the tape thickness. The minima of $V_{m_F}(\mathbf{x})$ form a periodic pattern above the tape surface, at a height $z_0 = k_M \ln(B_0/B_1)$. The spacing between two nearest minima along x is just the period of the magnetization $\delta x_M \equiv 2\pi/k_M$. From the series expansion of equation (49) along x for $\theta = 0$ around its minimum, we obtain for the anharmonicity parameter

$$\lambda = \frac{\pi^3 \hbar k_M}{\sqrt{m \mu_B B_2}} \left(\frac{B_1}{B_2} + \frac{B_2}{3B_1} \right) \tag{50}$$

which, for $2\pi k_M^{-1}$ around a few μm and for fields B_i of a couple hundred Gauss, is of the order of 10^{-3}.

8 Conclusions

In the present paper we have extended the investigations concerning the performance of a phase gate, as proposed by Calarco et al. in reference [3]. The phase gate employs cold trapped neutral atoms and the gate operation is obtained with internal state–selective trapping potentials that allow collisional interaction between the atoms.

A correct performance of quantum gates is an essential ingredient of a quantum computer. We have therefore relaxed the ideal conditions in reference [3] in order to check the tolerance of the proposed scheme to experimental imperfections. We have considered the effects of two possible sources of undesired disturbance, i.e., non-perfectly harmonic trapping potentials and temperature. The most crucial parameter is the trap anharmonicity λ. By studying the dependence of the gate fidelity on such parameter, we have been able to give a prescription to adjust other trap parameters as to compensate for this source of infidelity. However, we found a critical value for λ around 10^{-3} where the fidelity starts to be significantly degraded (i.e., well beyond any threshold for fault-tolerant quantum computation). This value turns out to be right on the edge of what can be presently achieved with magnetic micropotentials (atom chips). Thus a further optimization is needed.

The gate performance could be improved by changing the shape of the trapping potential during the gate operation. This requires the simultaneous variation of various physical parameters, λ, ω, ω_0, and $\omega_\perp$, since the fidelity depends on all these quantities. A viable approach to numerically search for improved solutions is given by quantum optimal control theory [21], and will be the subject of future investigations.

This work was performed with the support of the EC project ACQP (IST-2001-38863). M.A. Cirone and A. Negretti acknowledge partial financial support from the ESF program QIT. T. Calarco acknowledges support from the EU project "Cold Quantum Gases"; M.A. Cirone also acknowledges financial support from the EU-funded project QUEST and the friendly hospitality at ECT* in Trento. A. Negretti acknowledges the financial support provided through the European Community's Human Potential Programme under contract HPRN-CT-2002-00304, [FASTNet]. A. Negretti thanks

S. Bettelli and C. Henkel for very stimulating discussions and the friendly hospitality at Institut für Physik in Potsdam.

Appendix: Fidelity

We see how it is possible to calculate the minimum of the expression (45). Let us define the function

$$\mathcal{L}(x_\gamma) = \sum_{\alpha,\beta} x_\beta x_\alpha T_{\beta\alpha}, \tag{51}$$

where $x_\gamma = |c_\gamma|^2$ with the constraint given by the set of zeros of the function

$$\mathcal{G}(x_\gamma) = \sum_{\alpha} x_\alpha - 1. \tag{52}$$

Thus we have to solve the linear system of equations

$$\nabla\mathcal{L} - \lambda\nabla\mathcal{G} = 0. \tag{53}$$

that is,

$$M_{\alpha\beta}x_\beta = \lambda \qquad M_{\beta\alpha} = T_{\beta\alpha} + T_{\alpha\beta}. \tag{54}$$

The minimum of $\mathcal{L}$ is then

$$\begin{aligned}\mathcal{L} &= \frac{1}{2}\left[\sum_{\beta\alpha} x_\beta x_\alpha T_{\beta\alpha} + \sum_{\alpha\beta} x_\alpha x_\beta T_{\alpha\beta}\right] \\ &= \frac{1}{2}\sum_{\alpha\beta} x_\beta \left[T_{\beta\alpha} + T_{\alpha\beta}\right] x_\alpha \\ &= \frac{1}{2}\sum_{\beta} x_\beta \sum_{\alpha} M_{\beta\alpha}x_\alpha = \frac{1}{2}\sum_{\beta} x_\beta\lambda = \frac{\lambda}{2}.\end{aligned} \tag{55}$$

References

1. M.A. Nielsen, I.L. Chuang, *Quamtum Computation and Quantum Information* (Cambridge University Press, 2000)
2. J.I. Cirac, P. Zoller, Phys. Rev. Lett. **74**, 4091 (1995); Q.A. Turchette et al., Phys. Rev. Lett. **81**, 3631 (1998); T. Calarco, J.I. Cirac, P. Zoller, Phys. Rev. A **63**, 062304 (2001)
3. T. Calarco et al., Phys. Rev. A **61**, 022304 (2000)
4. Q.A. Turchette et al., Phys. Rev. Lett. **75**, 4710 (1995); X. Maitre et al., Phys. Rev. Lett. **79**, 769 (1997); E. Hagley et al., Phys. Rev. Lett. **79**, 1 (1997); T Pellizzari, S.A. Gardiner, J.I. Cirac, P. Zoller, Phys. Rev. Lett. **75**, 3788 (1995)
5. D.G. Cory, A.F. Fahmy, T.F. Havel, Proc. Natl. Acad. Sci. USA **94**, 1634 (1997); N.A. Gershenfeld, I.L. Chuang, Science **275**, 350 (1997)
6. See Fortschr. Phys. **48**, No. 9–11 (2000), special issue on quantum computing
7. A. Barenco et al., Phys. Rev. A **52**, 3457 (1995)
8. T. Busch et al., Found. Phys. **28**, 549 (1998)
9. M. Greiner et al., Nature **415**, 39 (2002)
10. N. Schlosser et al., Nature **411**, 1024 (2001); S. Bergamini et al., preprint `arXiv:quant-ph/0402020`
11. D.G. Grier, Nature **424**, 810 (2003)
12. R. Dumke et al., Phys. Rev. Lett. **89**, 220402 (2002)
13. R. Folman et al., Adv. At. Mol. Opt. Phys. **48**, 263 (2002)
14. M. Olshanii, Phys. Rev. Lett. **81**, 938 (1998)
15. D.S. Petrov et al., Phys. Rev. Lett. **85**, 3745 (2000)
16. M. Abramowitz, I.A. Stegun, *Handbook of mathematical functions* (Dover publications, New York, 1972)
17. B. Schumacher, Phys. Rev. A, **54**, 2614 (1996)
18. T.M. Roach et al., Phys. Rev. Lett. **75**, 629 (1995)
19. E.A. Hinds et al., Phys. Rev. Lett. **80**, 645 (1998)
20. E.A. Hinds, Philos. Trans. R. Soc. Lond. A **357**, 1409 (1999)
21. See, e.g., S. Sklarz, D. Tannor, Phys. Rev. A **66**, 53619 (2002)